Summary of professional accomplishments

1 Name

Krzysztof Aleksander Jachymski

2 Diplomas and scientific degrees

- **PhD degree in Physics**, University of Warsaw, Poland
  date: June 2015
  thesis title: *Quantum control of collisional properties of ultracold atoms and molecules*
  supervisor: dr hab. Zbigniew Idziaszek

- **M.Sc. degree in Physics**, University of Warsaw, Poland
  date: April 2011
  thesis title: *Statistical properties of ultracold quantum gases in disordered potentials*
  supervisor: dr hab. Zbigniew Idziaszek

3 Employment in research institutions

- Assistant Professor at Faculty of Physics, University of Warsaw, Poland
  since July 2020

- Postdoctoral Researcher at Forschungszentrum Jülich, Germany
  September 2018 - June 2020

- Postdoctoral Researcher at University of Stuttgart, Germany
  September 2015 - August 2018

- Postdoctoral Researcher at University of Warsaw, Poland
  July 2015 - August 2015

- PhD student, University of Warsaw, Poland
  May 2011 - June 2015

4 Description of the achievements set out in art. 219 par. 1 point 2 of the Act

4.1 Title of the scientific achievement

The achievement is a series of articles on the topic

Quantum engineering with compound ultracold atomic systems

4.2 List of publications constituting the achievement

H.1 G. Astrakharchik, L. Peña Ardila, R. Schmidt, K. Jachymski and Antonio Negretti, *Ionic polaron in a Bose-Einstein condensate*, accepted in Communications Physics (2021)

H.2 T. Dieterle, M. Berngruber, C. Hölzl, R. Löw, K. Jachymski, T. Pfau and F. Meinert, *Transport of a single cold ion immersed in a Bose-Einstein condensate*, Phys. Rev. Lett. 126, 033401 (2021)

H.3 T. Dieterle, M. Berngruber, C. Hölzl, R. Löw, K. Jachymski, T. Pfau and F. Meinert, *Inelastic collision dynamics of a single cold ion immersed in a Bose-Einstein condensate*, Phys. Rev. A 102, 041301(R) (2020)

H.4 K. Jachymski and A. Negretti, *Quantum simulation of extended polaron models using compound atom-ion systems*, Phys. Rev. Research 2, 033326 (2020)

H.5 K. Jachymski and F. Meinert, *Vibrational quenching of weakly bound molecular ions immersed in their parent gas*, Appl. Sci. 10(7), 2371 (2020)

H.6 K. Jachymski, *Precise Feshbach resonance spectroscopy using tight anharmonic traps*, J. Phys. B 53, 065302 (2020)

H.7 T. Wasak, K. Jachymski, T. Calarco, A. Negretti, *Magnetic gradiometer based on ultracold collisions*, Phys. Rev. A 97, 052701 (2018)

H.8 K. Jachymski, T. Wasak, Z. Idziaszek, P. S. Julienne, A. Negretti, T. Calarco, *Single-atom transistor as a precise magnetic field sensor*, Phys. Rev. Lett. 120, 013401 (2018)

H.9 R. Ołdziejewski, K. Jachymski, *Properties of strongly dipolar Bose gases beyond the Born approximation*, Phys. Rev. A 94, 063638 (2016)

H.10 K. Jachymski, *Impact of overlapping resonances on magnetoassociation of cold molecules in tight traps*, J. Phys. B 49, 195204 (2016)

Description of my contribution to these works is included in the List of scientific achievements (Appendix 5).

4.3 Detailed description of the achievement

Ultracold atomic systems are now a well established field at the interface of atomic and condensed matter physics [1]. Cooling ensembles of atoms all the way to the quantum degeneracy opens a number of unique opportunities for fundamental studies as well as potential applications. When thermal fluctuations are suppressed, collective quantum effects not only become observable, but often lead to qualitatively new phenomena. Atomic systems are now also considered as a promising platform for implementations of quantum technologies such as metrology, quantum information processing and quantum simulations [2]. This, however, requires very precise microscopic understanding of realistic experimental systems, which is challenging due to increasing complexity in currently developed experimental setups. A noticeable example are systems in which particles interact strongly over long distances due to the presence of free charges (ions) or having a dipole moment (e.g. lanthanide atoms). The presented series of articles explores different aspects of few-body physics needed to achieve this goal and make atomic systems useful for applications in the future. Specifically, papers [H10,H6] focus on increasing the accuracy of Feshbach resonance spectroscopy utilizing tight optical traps, which is relevant in particular for lanthanide atoms that feature extremely dense Feshbach spectra hard to resolve in traditional

three-body loss measurements. Article [H9] investigates the role of the interplay between dipolar and short-range interaction among magnetic atoms in the formation of the so-called quantum droplets. Then in works [H7,H8] a new scheme for measuring static magnetic fields with unprecedented precision and spatial resolution by means of Feshbach resonances is proposed. The next papers are focused on hybrid ion-atom systems. Firstly, works [H2,H3,H5] are concerned with the basic collisional properties of an ion moving in an ultracold gas, with a particular emphasis on transport and inelastic collisions. Article [H1] is dedicated to the many-body ground state of an ion placed in a degenerate bosonic gas. Finally, article [H4] studies the possibility for quantum simulation of realistic quantum materials with strong electron-phonon interaction using a hybrid ion-atom setup.

Before a more detailed description of the original results constituting the series, the following section provides a brief overview of the field which serves as a starting point for the subsequent discussion.

4.4 Introduction to ultracold atomic systems

From the point of view of a theoretical physicist, the research aimed at the properties of utracold quantum matter started already in 1920s, in particular with the prediction that noninteracting bosons can undergo a phase transition to a condensed state (Bose-Einstein condensate, BEC) with macroscopic occupation of the lowest lying eigenstate at finite temperature [3]. However, the emergence of collective quantum effects at low temperatures has been demonstrated experimentally already in 1911 with the discovery of superconductivity in solid mercury in the group of Heike Kammerlingh Onnes, although microscopic understanding of this phenomenon was lacking at that time [4]. The possible connections between superconductivity and Bose-Einstein condensation have triggered intense research which lead to the celebrated pairing model introduced by Bardeen, Cooper and Schieffer (BCS) [5]. Importantly, theoretical models of solid materials are extremely hard to verify in experiments due to limited access to the system and the necessity to rely on a limited set of available measurements which are often not directly connected to microscopic quantities. Real materials are also hard to manipulate and are characterized by very fast (subpicosecond) timescales. For these reasons, introducing pure and controllable atomic systems with better optical access as a complementary experimental platform can be very beneficial.

The development of laser technology completely revolutionised the research in quantum physics at several levels, bringing a huge number of breakthroughs in multiple fields beyond the scope of this short note. Crucially, it also enabled precise spectroscopy of atomic lines [6] and then optical trapping and cooling of atoms in the gas phase [7, 8]. This lead to the idea that atomic gases could be cooled to quantum degeneracy and realize the BEC phase. In 1978, Thomas Greytak and Daniel Kleppner from MIT began a 20-year endeavour towards this goal using atomic hydrogen. Realization of atomic BECs with alkali atoms turned out to be technically less challenging and condensates of sodium (group of Carl Wieman and Eric Cornell) and rubidium (group of Wolfgang Ketterle) were demonstrated in 1995 [9, 10], with hydrogen following in 1998 [11]. Since then, several more atomic species have been condensed, and degenerate Fermi gases have been produced as well. In these experiments, it was crucial to get detailed understanding of the atomic structure, interaction with electromagnetic fields and collisional properties via spectroscopy and theoretical calculations.

Alkali atoms (first group in the periodic table) have a considerably simple internal structure which allowed not only to design very efficient cooling protocols, but also to characterize their interactions with high accuracy. Recently, new systems involving other types of atoms [12], as well as ions [13] and molecules [14] with rich internal structure have drawn a lot of attention, offering a broad range of new possibilities but being harder to deal with both in experiment and theory. Every new systems comes with a unique set of challenges in terms of cooling and

trapping, interaction control, measurement protocols and scalability.

The fact that ultracold atomic systems are not just a peculiarity, but rather a vital research field can be attributed to unparalleled level of control achievable in these systems. Nowadays, practically all of the system parameters can be manipulated in real time, including the shape of the trapping potential, the number of particles, and the strength and sign of the effective inter-particle interactions. Moreover, they can be easily accessed optically, allowing for reconstruction of both the density and momentum distributions. This immediately brings to mind the idea of a quantum simulator often attributed to Richard Feynmann [15]. Having a versatile platform, one could imagine assembling quantum systems described with almost arbitrarily chosen Hamiltonians and studying both their ground state and dynamic properties. This would potentially allow for understanding complex quantum systems which are hard to tackle analytically and prohibitively expensive for classical computer simulations. A notable early example can be the realization of the Mott insulator to superfluid phase transition observed with rubidium atoms trapped in an optical lattice, which can be accurately described using Bose-Hubbard model [16]. Furthermore, realization of long-lived entangled many-body states would be beneficial for applications such as quantum-enhanced metrology [17].

4.5 Feshbach resonances in tight anharmonic traps

Feshbach (also called Fano-Feshbach) resonances are one of the most essential tools in ultracold atomic systems. They allow not only for controlling the interactions between the atoms, but also producing weakly bound molecules which can then be efficiently transferred to the ground state using Raman transitions [18]. The underlying principle of Feshbach resonances is quite general, as they have been originally predicted in nuclear physics [19]. Let us consider two separated atoms prepared in a well defined internal state such as a hyperfine level $|F, m_F\rangle$ with F denoting the total (electronic + nuclear) spin. The system can be described by the state vector $|F_1, F_2, m_{F1}, m_{F2}\rangle$. At small separation a more suitable basis is the molecular one $|I, J, m_I, m_J\rangle$, where I is the nuclear and J total electronic spin. Short-range interactions give rise to a difference between the molecular potentials depending on their symmetry, which effectively provides a coupling between the channels in the asymptotic free atom picture. This becomes especially important if there is a bound state in the energetically closed hyperfine channel with energy $E_c - E_{\mathrm{bnd}}$ (threshold energy of the closed channel minus the binding energy) similar to the energy in the initial state $E_o + E_{\mathrm{kin}}$ (threshold energy of the open channel plus the kinetic energy). Within a semiclassical picture the atoms will then approach each other, acquire some bound state character and create a long-lived resonance state before they separate again, leading to a large scattering phase shift. Crucially, the relative energy between the bound state and the threshold can be tuned by varying external magnetic field thanks to the differential Zeeman shift between different hyperfine levels. This also means that sweeping the magnetic field across the resonance can lead to creation of weakly bound molecules.

For collisions involving short-range interactions at very low energies a single partial wave is relevant, as the centrifugal barrier is much higher than the kinetic energy of the particles. It is then convenient to introduce the scattering length defined for s-wave interactions as

$$a(k) = -\frac{\tan \delta(k)}{k}\,, \tag{1}$$

where $\delta(k)$ is the scattering phase shift and the kinetic energy of the relative motion is $E = \hbar^2 k^2 / 2\mu$ with μ being the reduced mass. The interaction between neutral atoms can then be described by the pseudopotential $V(r) = a(k \to 0)\delta(r)\frac{\partial}{\partial r}(r\cdot)$ with the last part being necessary to regularize the wave function at short distance.. Close to the resonance the scattering length

at zero energy is described by a simple formula

$$a(B) = a_{\rm bg}\left(1 - \frac{\Delta}{B - B_{\rm res}}\right), \tag{2}$$

with $a_{\rm bg}$ being the background scattering length in the entrance channel away from the resonance, Δ denoting the resonance width and $B_{\rm res}$ its position. It is then in principle possible to tune the scattering length to arbitrary values by simply changing the magnetic field. An important quantity characterizing the resonance is its pole strength $s_{\rm res} = a_{\rm bg}\Delta\delta\mu$ with $\delta\mu$ being the magnetic moment difference between the channel states. Large $s_{\rm res}$ corresponds to open-channel-dominated resonance in which the occupation of the molecular state is low, making them more universal (less sensitive to the potential details).

Detection of Feshbach resonances is often performed by scanning the magnetic field and looking at the number of atoms lost from the trap as well as their thermalization rate. The dominant loss channel are three-body losses resulting from quick relaxation to deeply bound molecular states which releases a lot of kinetic energy. At the resonance the two-body complexes become long-lived, enhancing the probability of three-body events. However, this method has several limitations, such as low resolution, low efficiency of molecule production and the complicated nature of the three-body collision processes which inhibits the understanding of loss spectra. Much better precision can be reached if the atoms are initially trapped in pairs in a tight external trap, e.g. using an optical lattice or a tweezer. This eliminates all three-body effects and provides higher initial two-particle overlap due to confinement, which enhances the probability for reaching the molecular state [20, 21, 22]. The prerequisites for understanding the energy level structure of two trapped particles were provided in the seminal work of Busch *et al.* [23] who solved the problem of a harmonic trap and contact interaction. Various extensions of this model have been done since then, involving anisotropic confining potential and corrections to the contact interaction. Here we describe a multichannel calculation needed to understand the case of several overlapping resonances [H10]. Then, we consider an anharmonic double-well potential and discuss the additional opportunities arising from the coupling to molecular states in an excited center of mass mode [H6].

The calculation is performed using an effective model in which the closed channels are uncoupled after a pre-diagonalization. The Hamiltonian of the system reads

$$\begin{aligned} H = |o\rangle\langle o|\left(\frac{p^2}{2\mu} + \frac{P^2}{2M} + V(\mathbf{r},\mathbf{R})\right) + \\ + \sum_i |\chi_i\rangle\langle\chi_i|\left(\frac{P^2}{2M} + \tilde{V}(\mathbf{R})\right) + \sum_i \left(|\chi_i\rangle\langle o| W_i + \text{h.c.}\right), \end{aligned} \tag{3}$$

where $|o\rangle$ labels the open channel, $|\chi_i\rangle$ denotes the closed molecular channels, μ is the reduced mass of the pair, M is the total mass, p describes the relative momentum and P the center of mass momentum. Furthermore, $W_i(\mathbf{r}) = g_i\delta(\mathbf{r})$ describes the couplings and V, $\tilde{V}$ denote the trapping potential which may differ in general due to polarizability change. The coupling strength g can be linked to the individual resonance parameters by comparing the molecular energy in the limit of vanishing trap frequency to the free space case. The problem can be solved by decomposing the wave function into trap eigenstates ψ_n and Φ_N

$$|\Psi\rangle = |o\rangle\sum_n c_n\psi_n(\mathbf{r},\mathbf{R}) + \sum_i |\chi_i\rangle\sum_p a_p^i\Phi_p(\mathbf{R}), \tag{4}$$

and subsequent renormalization of the self-consistent equation for the eigenenergies. This allows to solve a wide class of problems including the case of many channels as well as an anisotropic harmonic trap semi-analytically. It turns out that closely spaced, overlapping bound states

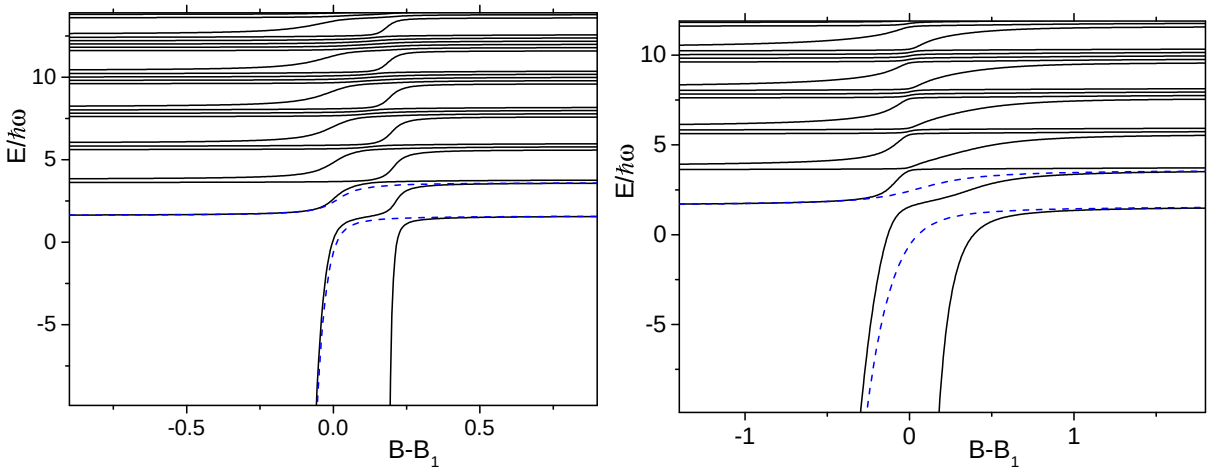

Figure 1: Two resonances in a slightly anisotropic trap ($\eta = 1.1$) with widths $\Delta_1 = 2.5$G and $\Delta_2 = 0.5$G, separated from each other by 0.3G. Left: $\omega = 250$Hz. Right: $\omega = 5$kHz. The blue dashed lines show the first two levels for the case in which there is only a single resonance present. From [H10].

have a number of interesting properties distinguishing them from the single resonance case. An illustrative example is provided in Figure 1, which shows two resonances separated by 0.3G for two different trapping frequencies. When the confining potential is weak, the resonances are clearly separated. As the trap gets stronger, the two molecular states get mixed with each other, and the bound state energy is shifted due to the presence of the second resonance. This has immediate practical implications for molecule production schemes, allowing for optimization of the trap frequency and the magnetic field ramp speed to achieve maximum fidelity. Otherwise, the process may be spoiled by populating multiple molecular states which will not be compatible with the subsequent laser pulse.

The treatment outlined above can also be applied to anharmonic traps after some careful adjustments. It is of particular interest to investigate the case of a double well trapping potential, naturally related to the optical lattice in which tunnelling between adjacent sites is allowed. In order to mimick the lattice potential $V(z) = V_L \cos^2 k_L z$ with lattice wavector k_L, one can use a model potential of the form

$$V(z) = V_L \left((zk_L)^2/a + \frac{4}{1 + (zk_L)^2/b + (zk_L)^4/c} \right) , \tag{5}$$

with parameters a, b, c fixed such that the first few terms in the Taylor expansion of the potential agree with the original one. In such a double well potential, the trap eigenstates come in almost degenerate pairs of even and odd symmetry and can be combined into states localized in either of the wells. Note that the potential now couples the center of mass and relative motion of the particles. As a result, many more states can be coupled with each other, resulting in processes such as creation of a motionally excited molecular state. This is visible in the energy diagram as anticrossings between the states with different number of center of mass excitations. Such features are detectable in experiment, causing extremely sharp loss peaks [20]. The crucial observation of work [H6] is that the positions of these new narrow resonances depend on the $s_{\rm res}$ parameter, meaning that one can detect not only the resonance position but also characterize its pole strength. The dependence of the narrow resonance positions on $s_{\rm res}$ can be understood as a result of effective range corrections to the formula (2). Low energy expansion of the scattering phase shift reads $k \cot \delta(k) = -\frac{1}{a} + \frac{1}{2} r_{\rm eff} k^2 + \dots$ with the effective range given by $r_{\rm eff} = -\frac{\hbar^2}{\mu a_{\rm bg} \Delta\delta\mu}(1 - \frac{a_{\rm bg}}{a(B)})^2$ [24]. Clearly, as the effective range depends on the inverse of $s_{\rm res}$,

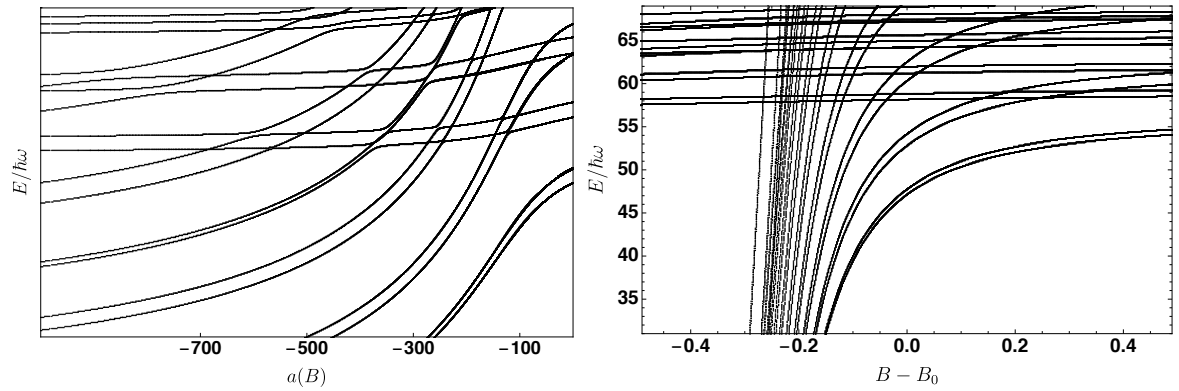

Figure 2: Left: crossings of the molecular levels with the first few trap states for a closed-channel-dominated Feshbach resonance. Right: The case of a wide (open-channel-dominated) resonance. From [H6].

it will lead to differences in the couplings for excited states which have finite energy. This also means that the effects will be more pronounced for tight traps in which the zero point motion $\hbar\omega$ is larger. An exemplary energy spectrum for a narrow resonance is shown in Figure 2. Here the contribution of the molecular level is very large, inducing strong anticrossings which would be observed in experiment as a dense loss spectrum.

The formalism presented in this section is highly general and applicable to the case of tight trapping potentials such as optical tweezers which are the new emerging system for controlled production and coherent manipulation of cold molecules.

4.6 Dipolar scattering beyond the Born approximation

Recently developed experimental platforms based on ultracold lanthanide atoms such as erbium and dysprosium revolutionized the field, allowing to investigate the role of long-range interactions in determining the gas properties. These atomic species feature an open electronic shell, giving rise to high magnetic moment and consequently strong dipolar interactions [12]. Complex internal structure of these atoms, including high spin and anisotropic van der Waals couplings, leads to extremely high density of Feshbach resonances, representing an additional challenge both for theory and experiments. Even in the limit of weak interactions, the properties of a dilute dipolar Bose gas are highly affected by the long-range and anisotropic nature of the dipole-dipole interaction term. For example, the Bogoliubov excitation spectrum can acquire unstable modes and cause the gas to collapse [25]. Even more striking effects where observed in 2016 in the group of prof. Tilman Pfau, when stability of the dysprosium condensate has been investigated. Instead of collapsing, the gas formed a set of long-lived finite-sized droplets with relatively high density [26]. It is noteworthy that at the time there was no such theoretical prediction and the experimental group made this discovery rather spontaneously. This effect was then attributed to beyond-mean-field corrections to the equation of state, which induce additional repulsion required to stabilize the system [27]. The functional form of these corrections for a homogeneous dipolar gas is analogous to the Lee-Huang-Yang term known for contact interactions and can be calculated in a straightforward fashion [28]. However, multiple effects not taken into account in the simplified theoretical models can impact the stability boundary and the droplet properties. One aspect of the problem is the effective potential used in the calculations. The usual mean-field treatment relies here on the low energy scattering amplitude $f(\theta)$ which may depend on the relative angle between the dipole moment orientation and the interparticle axis θ. In the case of dipolar scattering it is required to include many partial waves

in its calculation. In principle, the Born approximation $f_B(\theta) = -\frac{2\mu}{\hbar^2}\frac{1}{4\pi}\int d^3r\, e^{iqr}V(r)$ can be used for this purpose [29], leading at vanishing momentum q to a simple formula

$$f_B(\theta) = -a - R_{\rm dd}P_2(\cos\theta)\,, \tag{6}$$

where a is the s-wave scattering length of the full potential (taking into account the corrections from the dipolar interaction), P_2 is the Legendre polynomial and the dipolar interaction strength is described in terms of characteristic length $R_{\rm dd} = 2\mu d^2/3\hbar^2$ with d being the dipole moment. One can also define the corresponding characteristic energy $E_{\rm dd} = \hbar^2/(2\mu R_{\rm dd}^2)$.

However, for lanthanide atoms the validity of the Born approximation can be limited due to the competition between short- and long-range interactions, especially in the vicinity of resonances which are ubiquitous in these systems. Furthermore, although the Born approximation for a pure dipolar potential becomes exact at zero energy, one can expect corrections to arise once $E_{\rm kin} \sim E_{\rm dd}$. These arguments motivate a numerical study of the scattering amplitude at realistic experimental conditions which has been performed in [H9]. In the calculations, a model potential consisting of isotropic van der Waals interaction and a dipolar part were combined. The scattering length could be varied by imposing different short-range boundary conditions on the wave function, mimicking the physics of an open channel dominated Feshbach resonance.

The calculations revealed that the numerically calculated scattering amplitude can be described with a formula which has the same form as in Eq. (6), but with modified dipolar length parameter $a_{\rm dd}$ instead of $R_{\rm dd}$. At moderate scattering length values this effective dipole length is a few percent larger than the standard one, depending on the collision energy. Approaching a scattering resonance leads to a significant deviation from the Born approximation predictions and strong reduction of the effective $a_{\rm dd}$. This can be explained by reckoning that close to the resonance the scattering is dominated by the extended quasibound state in the isotropic s-wave channel, reducing the anisotropy of the total scattering amplitude. Figure 3 shows the dependence of the effective dipolar length on the ratio $R_{\rm dd}/a = \epsilon_{\rm dd}$.

The simple correction to the effective potential suggested here allowed to slightly improve the agreement between the experiment and theory in predicting the stability boundary of the quantum droplets [30]. The treatment of the droplet employed in [H9] made use of the standard extended Gross-Pitaevskii functional which utilizes the analytically derived beyond mean field correction for a homogeneous gas, neglecting the finite size of the droplet, and a simple gaussian variational ansatz. The validity of these approximations is naturally quite restricted.

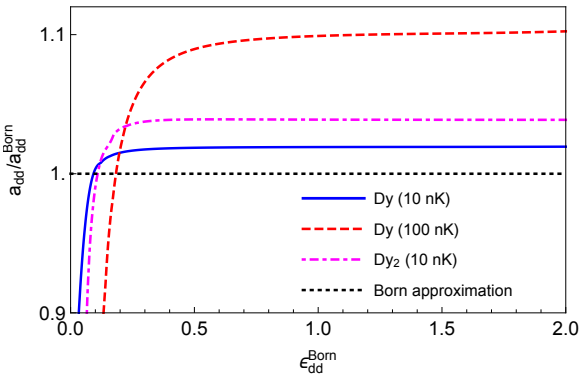

Figure 3: Effective dipolar length as a function of $\epsilon_{\rm dd}$ for dysprosium atoms at 10nK (blue straight line) and at 100nK (red dashed line) collision energy, as well as for Dy_2 (dot-dashed magenta line). Dotted black line shows the Born approximation result $a_{\rm dd}/R_{\rm dd} = 1$. From [H9].

4.7 Magnetometry with ultracold collisions

In section 4.5 it has been demonstrated that strong confinement can increase the achievable precision and magnetic field resolution due to elimination of three-body events and increased two-body wavefunction overlap. This allows for tuning interparticle interactions with high accuracy. Works [H7,H8] analyze a reverse problem - can one use the information obtained from

scattering measurements to deduce the value of the magnetic field, and how competitive would such a sensor be? One should note at this point that magnetometry techniques based on cold atomic vapors taking advantage e.g. of Faraday rotation are already established, but interactions in theses systems are negligible. As it turns out, a direct scattering length measurement based on the many-body dynamics of an ultracold gas or three-body losses would be rather inefficient, require long operation times and cannot provide satisfactory resolution. However, restricting to the case of pairs of particles in a tight external trap allows for significant improvement, as described below.

The sensor idea is based on reduced dimensional scattering taking place in tubes, which can be created by two pairs of laser standing waves. In the center of every waveguide there is a static impurity on which the incident atoms will scatter. For low enough kinetic energy, in 1D geometry the atom has only two possibilities after the collision: it can be transmitted or reflected, as excitations of transverse oscillator modes are not allowed. This also means that in quasi-1D there are only two partial wave analogs: the even and odd wave, with respective scattering amplitudes denoted as $f^{(\pm)}$ reflecting the symmetry of the state. The natural quantity to measure is then the transmission amplitude which describes the part of the flux that goes through the waveguide, defined as

$$T(p) = \left|1 + f^{(+)} + f^{(-)}\right|^2 , \tag{7}$$

with p denoting the 1D wavenumber. The outcome of the collision can be monitored experimentally e.g. by field ionization or absorption imaging, and the sensitivity to magnetic field is naturally provided by the Feshbach resonance. Additionally, the separation between the tubes, which for optical lattices can be of the order of 500nm, gives rise to high spatial resolution.

The basic formalism for theoretical description of scattering in quasi-1D geometry has been provided by Maxim Olshanii [31]. The problem can be dealt with by solving the three-dimensional stationary Schrödinger equation involving the interaction and confinement with the proper boundary conditions. The interaction can be described by a set of pseudopotentials which contain the information about the 3D scattering phase shifts in all partial waves. Crucially, the external trap impacts the collision by shifting the position of the resonance to finite values of the 3D scattering length, a phenomenon which is called confinement-induced resonance (CIR). Furthermore, all even 3D partial waves $\ell = 0, 2, \ldots$ lead to emergence of resonances in the even 1D scattering amplitude, while odd angular momenta induce resonances in the odd wave due to symmetry. As an illustration, figure 4 shows the examplary magnetic field dependence of the 3D scattering lengths corresponding to the first few partial waves for an exemplary Feshbach resonance characterized by the width $\Delta = 0.1$G. The resulting transmission profiles are then shown in Figure 5. Here we use the unit of length corresponding to the characteristic van der Waals distance $\bar{a}$, defined as the mean scattering length of the $-C_6/r^6$ potential after averaging over the short-range phase.

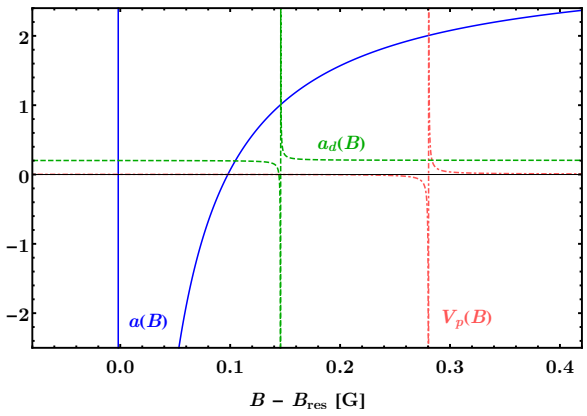

Figure 4: The s-wave scattering length, p-wave volume and d-wave length for an exemplary Feshbach resonance with 0.1G width and high background scattering length. From [H7].

Let us now discuss the achievable precision of the sensor. Intuitively, it is beneficial to work in the proximity of a resonance, as then the dependence of transmission on magnetic field is

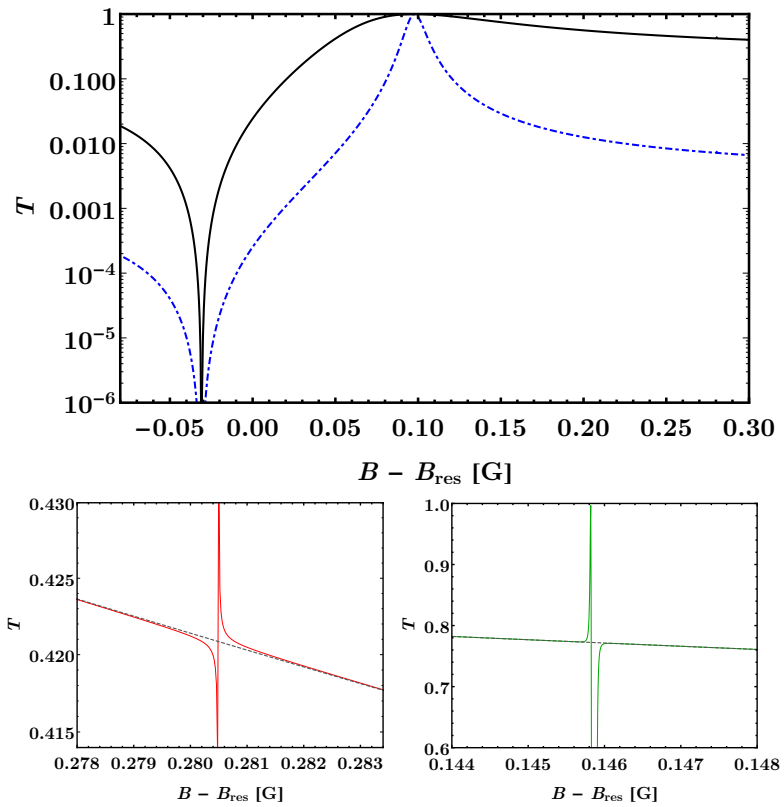

Figure 5: Transmission coefficient as a function of magnetic field for the same s-wave resonance as in Fig. 4, for $p = 0.01\bar{a}^{-1}$ (black solid line) and $p = 0.001\bar{a}^{-1}$ (blue dash-dotted line). The narrow resonances caused by higher partial wave scattering are not visible, but are shown in the lower panel for $p = 0.01\bar{a}^{-1}$. The dashed (black) line gives the s-wave result, while the straight lines include higher partial waves, i.e. p-wave on the left (red solid line) and d-wave on the right (green solid line). From [H7].

the strongest. This can easily be made formal by using parameter estimation theory [32, 33]. The minimum attainable uncertainty of the estimated field value is by definition given by the Cramer-Rao bound

$$\Delta B \geq \frac{1}{\sqrt{N}} \frac{1}{\sqrt{F}}\,, \tag{8}$$

where N is the number of atoms injected into the tube. Here the scaling $N^{-1/2}$ is merely a statistical factor (shot noise). The real figure of merit is given by the Fisher information F that is defined as

$$F = \sum_{s=\pm 1} \frac{1}{p(s|B)} \left(\frac{\partial p(s|B)}{\partial B} \right)^2 . \tag{9}$$

Here, $p(+1|B) \equiv T(B)$ is the transmission probability, and $p(-1|B) \equiv 1 - T(B)$ is the probability of reflecting the atom in the collision. It quickly follows that

$$F = \frac{1}{T(B)[1-T(B)]} \left(\frac{dT(B)}{dB} \right)^2 . \tag{10}$$

The formula (10) implies that the lowest uncertainty is indeed reached when the derivative of the transmission coefficient is the largest. The optimization of other parameters turns out to be nontrivial and depend on the nature of the resonance. Depending on the value of the background scattering length, the precision has a different dependence on the collision energy and it can take the highest values either at the CIR or at the unit transmission peak, as shown in Figure 6. This can be explained by extracting the leading order behavior of Eq. (10) at low energy. One finds that ΔB always scales linearly with the resonance width Δ. However, at the CIR a low background scattering length and a certain finite p is preferred, while at the unit transmission peak a high $a_{\rm bg}$ and a very low energy gives better results. The dependence on the background scattering length is not surprising, as one can expect that a jump in transmission should be preferable; consequently, e.g. from high values at low background to zero at the CIR.

Additionally, due to the structure of the optical lattice one can study the transmission in different tubes and obtain information about the spatial distribution of the field with the resolution given by the tube spacing, which is equal to half the laser wavelength, typically 532nm. For the field gradient estimation one can generalize the previous results by introducing a random variable $\boldsymbol{\xi} = \{\xi_1, \ldots, \xi_M\}$ describing the outcome of separate collisions taking place in M tubes. Let us also express slowly varying magnetic field in the plane of our interest as

$$B(\xi_i) = B_0 + B_x x_i + B_y y_i\,, \tag{11}$$

and we are interested in estimating all three parameters in this expression. Multiparameter estimation theory provides then an analogue of the Cramer-Rao bound involving the Fisher information matrix

$$\mathbf{C} \geqslant \frac{1}{N} \mathbf{F}^{-1}, \tag{12}$$

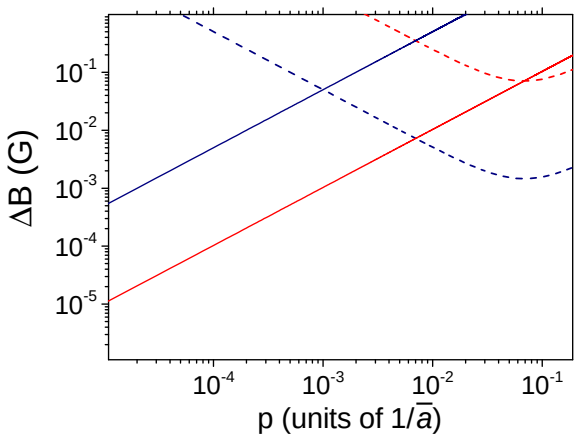

Figure 6: Estimation precision ΔB as a function of momentum for measuring at the CIR position (dashed lines) and the unit transmission peak (solid lines) for $a_{\rm bg} = 9.7\bar{a}$ (red) and $a_{\rm bg} = 0.2\bar{a}$ (blue). From [H8].

whose elements are given by

$$F_{i,j} = \sum_{\boldsymbol{\xi}} \frac{1}{p(\boldsymbol{\xi}|\boldsymbol{\gamma})} \frac{\partial p(\boldsymbol{\xi}|\boldsymbol{\gamma})}{\partial \gamma_i} \frac{\partial p(\boldsymbol{\xi}|\boldsymbol{\gamma})}{\partial \gamma_j}. \tag{13}$$

Figure 7 shows the minimal attainable uncertainty ΔB_x for the estimation of the magnetic field gradient along the x direction. The optimal operating point is achieved when $B_0 \approx \Delta$ and $B_x = 0$, and the sensor works best for small gradients. Interestingly, the precision ΔB_x oscillates as a function of the magnetic field B_0. The period of this wavy behaviour is decreasing as the gradient increases. This phenomenon has an intuitive explanation. If the gradient is zero and the sensor is working around its optimal operating point, all the tubes contribute with a small uncertainty. When the gradient is small, the local field at some of the waveguides departs from optimal conditions and the uncertainty of estimation grows. As the field strength B_0 is varied, the local field at some of the tube positions can incidentally approach the optimal point again. As a result, both ΔB_0 and ΔB_x do not reach the optimal point at finite gradient, but instead exhibit periodic behavior.

In the sensor implementation one would need to battle a number of potential error sources. One limiting factor is the finite width of the longitudinal momentum distribution. In addition, one has to consider variation of the resonance position due to finite energy corrections. Furthermore, the uncertainty of the estimated magnetic field strength depends on the efficiency of the detector, denoted by $0 \leqslant \eta \leqslant 1$.If the probability of detecting the transmitted (reflected) atom is given by $\eta P(\pm 1|B)$, the Fisher information simply reduces to $F^{(\mathrm{I})} = \eta F$, where F is the Fisher information for the perfect detectors. If the experimental setup only allows for monitoring the transmitted atoms, the Fisher information is instead given by $F^{(\mathrm{II})} = \eta(T'(B))^2/T(1 - \eta T(B))$.

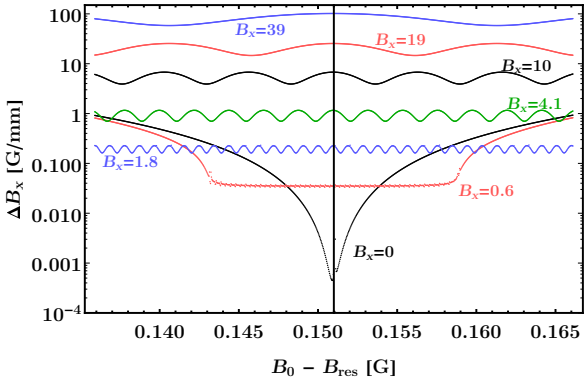

Figure 7: Gradient estimation uncertainty ΔB_x as a function of $B_0 - B_{\mathrm{res}}$ for fixed B_x. The black vertical line presents $B_0 - B_{\mathrm{res}} = \Delta$. The parameters used in the calculation were $\Delta = 0.15$G, transverse oscillator width $d = 20\bar{a}$, $a_{\mathrm{bg}} = 9.76\bar{a}$ (similar to Cs atoms) and $p = 10^{-4}\bar{a}^{-1}$. From [H7].

Finally, it is worth considering whether one can improve the performance of the sensor by utilizing a different measurement than just transmission. Surprisingly, the answer to this question is negative, as it is possible to show that the proposed scheme saturates the absolute bound taking into account all possible measurements. This follows from the structure of the scattering wave function in quasi-1D geometry. After the collision the particle is in a superposition of being transmitted or reflected with respective probability amplitudes. The modulus and phase of these amplitudes depend on the magnetic field. Our measurement scheme is only sensitive to the modulus square of the amplitudes. However, the phases of the amplitudes are equal and form a common phase factor. As a consequence, in our situation, the full information about the magnetic field is already contained in the moduli.

The detection scheme proposed here in principle allows for reaching subnanotesla, or about 100 pT/Hz$^{1/2}$ sensitivity at submicrometer resolution working with static magnetic fields. This quite unique combination is possible thanks to the high purity and controlability of atomic systems.

4.8 Collisional dynamics of an ion immersed in a cold bosonic gas

A further intriguing system in which the details of interparticle interactions can become important involves mixtures of cold atoms and ions. In this case the leading term in the interaction potential stems from the polarization of the atom by the charge of the ion and has $1/r^4$ dependence. Such potential has a well defined scattering length and approaches the s-wave limit at sufficiently low energies. However, this limit is extremely challenging to reach in experiment and instead one needs to take at least several partial waves into account. Here it is useful to introduce the characteristic interaction distance $R^\star = (2\mu C_4/\hbar^2)^{1/2}$ and the corresponding energy scale $E^\star = \hbar^2/(2\mu(R^\star)^2)$ where μ is the reduced mass. This energy is typically in the nK regime, and the $R^\star$ parameter can easily reach few thousands of Bohr radii and become comparable to the typical interparticle distance in the gas. Finally, corrections to the s-wave phase shift for the polarization potential are significant and feature terms which go beyond the effective range treatment, which has widely studied consequences especially in the context of electron-atom collisions [34]. A comprehensive review of the emerging field of cold hybrid ion-atom systems has been provided in [13].

The problem of a single ion immersed into a gas of ultracold bosons can be considered on various levels. One basic question concerns the transport properties resulting from elastic collisions with the surrounding atoms. However, inelastic events leading to charge transfer are also possible. Further relevant processes inculde radiative association of a molecular product as well three-body recombination. If a molecule is created, it can undergo dissociation as well as a secondary inelastic collision changing its rovibrational state.The complexity of the problem in the lab can be further increased by the presence of electromagnetic fields such as the trapping lasers which lead to additional processes, as well as stray electric fields which accelerate the ion. In a remarkable experiment [H2,H3], the group lead by Florian Meinert in Stuttgart has been able to create an ion from a cold Rb gas and monitor its collisional dynamics to some extent, obtaining valuable data.

After creation of the ion from the ultracold gas of rubidium atoms using a pulsed field-ionization process, it was dragged through the BEC by using very stable and weak electric field of a few mV/cm. After some waiting time, the ion was extracted from the gas by a strong electric field pulse and accelerated towards a detector. The ion arrival time allowed to estimate the distance that the ion traveled through the gas and deduce its drift velocity $\langle v_i \rangle$ and consequently its mobility $\mu_i = \partial\langle v_i\rangle/\partial E$ as a function of the applied weak field E. The results were then compared with a numerical simulation aiming to reproduce the observations without any free parameters. In the numerics, the ion motion has been modeled in a Monte-Carlo fashion, where the ion randomly scatters from the atoms with the energy-dependent collision rate. Each collision leads to a new ion trajectory with the scattering angle which is chosen from the appropriate distribution. This allows to include the finite size and inhomogeneous density profile of the gas.

The measured mobility value $\mu_i^{\rm exp} = (47 \pm 16) \times 10^3 {\rm cm}^2/({\rm Vs})$ turns out to be close to the numerical simulation outcome $\mu_i^{\rm num} = (33 \pm 3) \times 10^3 {\rm cm}^2/({\rm Vs})$, but systematically larger. As this is an initial study, both the experimental accuracy (e.g. stray field control) and theoretical assumptions for the model can be improved further. For instance, in the model the impact of inelastic processes and their density dependence has been completely disregarded. As we show in the next section, production of molecules due to three-body events also plays an important role in the ion dynamics.

The second set of measurements, described in [H3], focused on detection of the possible outcomes of inelastic processes. The ion detector could distinguish Rb+ from RB_2^+ ions by time of flight mass spectrometry, and indeed in a number of events the molecular ion has been detected, arriving at the detector at much larger times. This can only be due to three-body

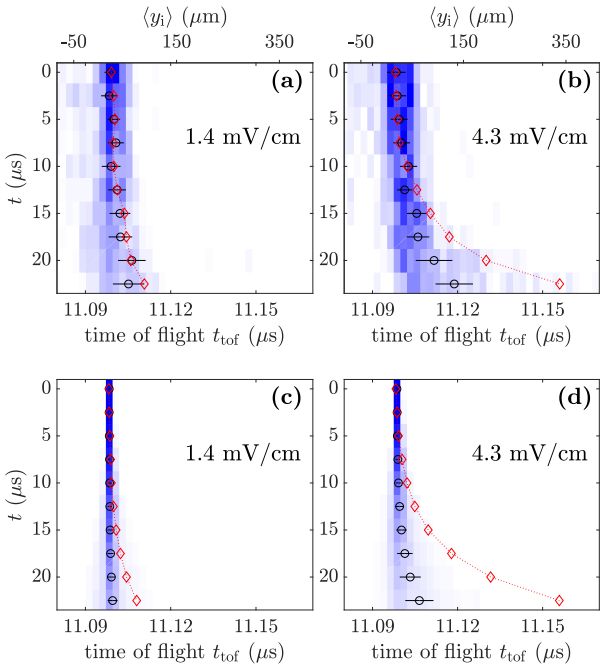

Figure 8: Measured (top row) and simulated (bottom row) distributions of the ion time of flight to the detector t_{tof} as a function of the transport time t for two electric field values. The color encodes the ion signal, while the black circles show the mean values. The red diamonds describe ballistic ion dynamics at vanishing atomic density. From [H2].

recombination events in which the ion captures an atom from the gas and forms a molecule. A unique experimental insight into the molecular products has been obtained by exposing them to an additional electric field pulse $\mathcal{E}_{\mathrm{ex}}$, which could dissociate them if their binding energy would be sufficiently low. The fraction of detected molecules thus provides information about the population of molecules with binding energies larger than the critical value. This allowed to reveal the collisional dynamics of the molecule after its creation, as different results were observed as a function of time. Namely, longer waiting times resulted in higher population of deeply bound states. This can be interpreted as follows: initially, the molecule is created in a rather loosely bound state. Subsequently, it undergoes secondary collisions with the neutral atoms which can be inelastic and change the rovibrational quantum state of the molecules. Incorporating the possibility of inelastic processes in the numerical simulation showed reasonable agreement with the experimental data.

Vibrationally inelastic collisions of homonuclear molecular ions with their parent atoms have been the subject of the work [H5], on which the analysis presented in [H3] is partially based. The three-body ion-atom-atom problem is in principle challenging to treat strictly. However, it is possible to take advantage from the long range properties of the ion-atom interaction to simplify it, which should work especially well at low collision energies. It is convenient to introduce the Jacobi coordinates and denote the relative position vector between the center of mass of the molecule and the atom by $\mathbf{R}$, and the internal coordinates of the molecular ion as $\mathbf{r}$. The center of mass motion is naturally eliminated. Furthermore, at large distances the system can by asymptotically described by the molecular ion in a rovibrational state $\phi_{vj}(r)$, where v and j label the vibrational and rotational quantum number of the molecule, respectively. In this basis

one can now calculate the potential matrix

$$W^{JM}_{vj,v'j'}(R) = \left(\frac{2\mu^\star}{\hbar^2}E_{vj} + \frac{\ell(\ell+1)}{R^2}\right)\delta_{vv'}\delta_{jj'} + \frac{2\mu^\star}{\hbar^2}V^M_{vj,v'j'}(R)\,, \tag{14}$$

with the matrix element

$$V^M_{vj,v'j'}(R) = 2\pi\int \phi_{v'j'}(r)Y_{j'M}(\gamma,0)V(R,r,\gamma)\phi_{vj}(r)Y_{jM}(\gamma,0)\sin(\gamma)d\gamma dr \tag{15}$$

containing the interaction between the free atom and the molecule. It then turns out that the diagonal potentials follow the same R^{-4} power law as the ion-atom interaction with minor short-range corrections. This suggests that the dynamics of the three-body complex should be at least partially universal, i.e. independent of the higher order terms. In a similar manner, the coupling terms which are responsible for inelastic processes also turn out to follow the $1/R^4$ dependence with an effective coupling strength depending on the molecular states involved. Only for the weakly bound states, which are spatially extended, the potential curves can deviate from this behavior, and the details of the effective interaction which determine the exact locations e.g. of the wave function nodes can become important.

As the interchannel couplings calculated using the above method are much weaker than the diagonal terms, it is warranted to use the distorted wave Born approximation (DWBA) to estimate the reactive collision rates instead of solving the problem in full. Within DWBA one makes use of the exact solution of the diagonal part of the problem and treats the inelastic processes perturbatively [35]. The result of the calculation is the distribution of molecular products after the collision. The obtained distributions for two different initial states ares shown in Fig. 10. In both cases small internal energy transfer is preferred. The collision rates and product distributions calculated this way were used as an input for the numerical simulation of the experiment shown in Figure 9.

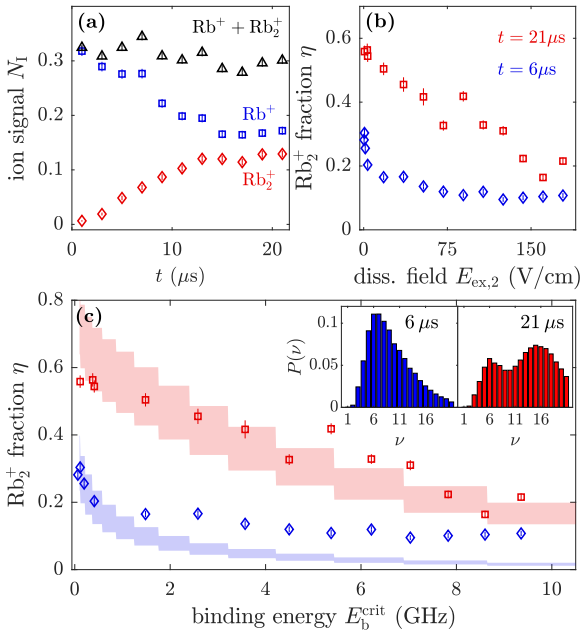

Figure 9: (a) Ionic and molecular signal as a function of the transport time. (b) Fraction of the detected molecules as a function of the dissociating field strength. (c) Fraction of the molecules which survive the dissociating field η as a function of the critical binding energy for two different evolution times $t = 6\mu$s (blue diamonds) and $t = 21\mu$s (red squares). The insets show the numerically calculated population distribution of the vibrational bound states for the two cases. From [H3].

4.9 Ionic polaron in a degenerate Bose gas

The previous section focused on the diffusive motion of the ion in a gas driven by two-body collisions. However, it is well known that the ground state of an impurity placed in a cold environment can have a many-body nature. The particle may become dressed with the elementary excitations of the medium, forming a polaron which can be characterized e.g. by a change in

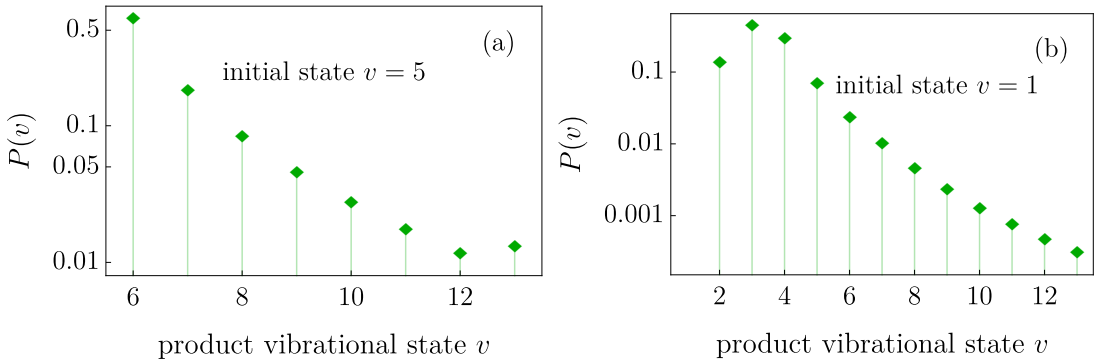

Figure 10: (a) Distribution of product states for vanishing kinetic energy after the inelastic collision for the 5th vibrational state ($v = 5$). (b) Same, but for the most weakly bound state ($v = 1$). From [H5].

the effective mass [36]. This problem is very appealing to a theoretician, as it can be seen as a building block for condensed matter systems and a testbed for different models. Since the first experimental observations [37, 38], the research on polaron physics using ultracold atoms is flourishing [39, 40]. It is then natural to ask whether charged particles can lead to new effects. As already noted, the ion-atom interaction is in principle short-ranged, so in a zero-temperature ultradilute gas the charged polaron would not differ from the neutral one. However, in typical experiments the competition of length and energy scales describing the interaction and the gas becomes important.

Let us first briefly consider the mean-field picture [41, 42, 43]. A single atom can form a two-body bound state with the ion, which would be roughly of the size of $R^\star$. An additional atom from the gas can also populate this bound state. Due to bosonic statistics, this only increases the interaction energy a little bit, and the binding energy is much greater. It is thus favorable to populate the molecular state with many more bosons, resulting in a cluster consisting of thousands of atoms trapped by the polarization potential. Such many-body state would have a very large effective mass and thus its diffusive motion would be much slower. However, the gas density in the proximity of the ion would greatly increase, so one can suspect that the mean field theory would no longer be applicable. Precise description of such a strongly correlated state is necessarily restricted to numerical studies. The calculations in the work [H1] were performed using variational and diffusion Monte Carlo methods which were benchmarked on short-range interacting systems and carefully adapted to the ion-atom case. In order to ensure convergence of the calculations, a model interaction potential regularized at short distances has been used, retaining the power-law long-range tail and allowing to control the number of available two-body bound states.

The crucial results of the study [H1] can be summarized as follows. If the ion-atom potential supports a bound state, the ground state of the system indeed corresponds to a large number of atoms bound to the ion. However, due to the density increase and boson-boson repulsion the critical number of atoms which can become bound N_c is much smaller than the mean field prediction. This number is in fact of the order of 100 and only weakly depends on the scattering length, which shows the important role of the universal long-range potential tail. The excess atoms remain in the gas phase. This is illustrated in Figure 11 with the two-body correlation functions. Naturally, the ion-atom correlation exhibits a large peak at short distances. The atom-atom correlation function exhibits the same behavior as the atoms tend to group around the ion and so remain also close to each other. This may also be interpreted in terms of impurity-induced interactions in the medium. If the number of bosons is less than critical, all of them are bound and at large interatomic distances the correlation drops to zero. Above N_c the atom-atom

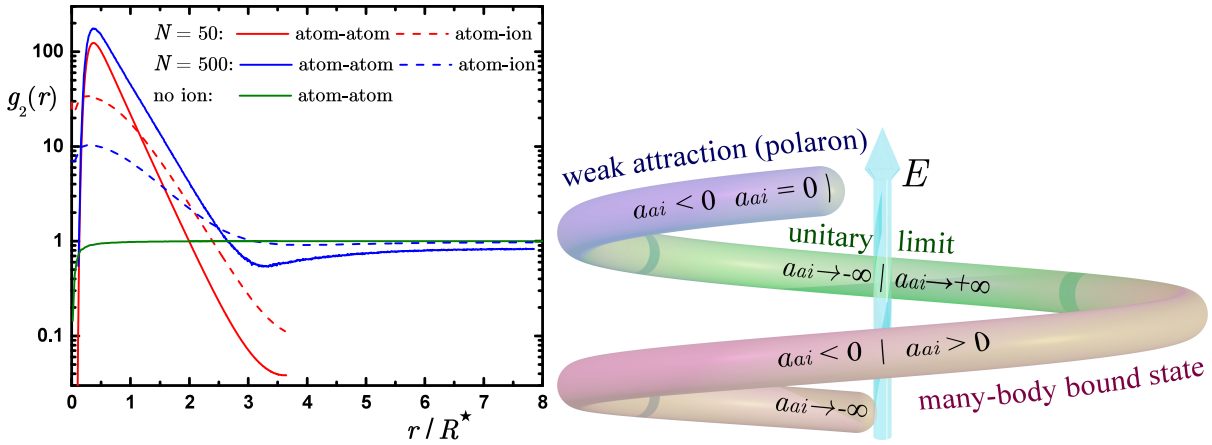

Figure 11: Left: Atom-atom (solid lines) and atom-ion (dashed lines) two-body correlation function for N = 500 (blue) and N = 50 (red). The two-body scattering length is chosen to be equal to $R^\star$. The green line is the correlation function of the bosonic gas in absence of the ion. Right: schematic picture indicating the different regimes the system can reach depending on the scattering length and the number of bound states. From [H1].

correlation converges to a constant smaller than unity, which reflects the reduced gas density as a fraction of atoms occupies the many-body bound state.

If a two-body bound state is not present, the many-body bound state cannot be formed as well. In this case the system turns out to be well described by the conventional attractive polaron theory, where the ion is dressed by the phonons and forms a quasiparticle with large residue, but small effective mass. Note that for the same negative scattering length but in the presence of a bound state the system will again form the mesoscopic molecular state. These two distinct regimes should give rise to different timescales in the impurity dynamics observed in experiment.

4.10 Quantum simulations with hybrid ion-atom systems

Ultracold atomic systems are often considered to be perfect candidates for the purpose of quantum simulations. The basic idea is to prepare a highly controllable and scalable system which would be able to realize complex many-body phenomena. In this way one would be able to study the properties of complex systems which are hardly accessible in experiments and cannot be efficiently simulated with a classical computer. This is especially promising in the context of out-of-equilibrium dynamics, but even ground state properties in the presence of competing processes and strong interactions can represent a challenge for theoretical understanding. One notable example here involves the interplay of strong electron-electron interactions and electron-phonon coupling observed in certain materials. As both processes naturally emerge in condensed matter systems, they have been a subject of intense theoretical studies for a long time [44, 45, 46]. It has been proposed that their competition can lead to a superconducting phase [47]. One can picture this by introducing lattice polarons, which are electrons dressed by phonons due to the strong coupling. The effective interaction between the polarons gives rise to bound states (bipolarons) which can have low effective mass and thus be mobile. Low mass indicates high condensation temperature and a possible collective quantum state. However, the theoretical treatment of such models including the details of the material structure is extremely challenging. Experimental efforts are also limited in that regard, as realistic material samples cannot be easily controlled, their dynamics is fast on optical scales and the measurement techniques are naturally limited to certain quantities such as conductance. Quantum simulation

utilizing an artificial system with well controlled properties and broad access to both local and global observables can thus become particularly useful in this context.

An ion crystal overlapping spatially with an atomic cloud naturally resembles a solid state material, with the atoms playing the role of electrons [48]. The ion-atom interaction provides a periodic potential for the atoms with a corresponding band structure. While microscopic details are different, the effective Hamiltonian describing the two systems can be made similar, with additionally controllable mass ratio and the energy scales involved in the problem. Furthermore, a trapped ion crystal can undergo a structural phase transition, e.g. a linear crystal can be destabliized by changing the effective confinement strength and enter a zigzag phase [49]. This phase transition can be controlled by using an atomic cloud which deconfines the ions due to the attractive potential. A natural question to ask is if it is also possible to realize a scenario in which the coupling to crystal phonons would become important. This was the motivation of the study performed in [H4], in which a linear crystal of ions directly overlapping with fermionic atoms has been considered. The system can be divided into three parts representing the ion chain, the atoms moving in the effective potential and their interaction with the phonons. Due to the fact that Coulomb interaction between the ions is strong and the ions are assumed to be heavier than the atoms, a reasonable assumption is to make use of the Born-Oppenheimer approximation in which the phonon structure is unperturbed by the atoms. For typical experimental parameters, the ions can be treated as classical distinguishable particles. In the first step, one can then minimize the classical energy functional with respect to the ion positions in order to obtain the lowest energy equilibrium configuration. The functional describes the interaction potential of the ion trap and the Coulomb repulsion, and their interplay can give rise to various geometries. Here, a stable linear configuration is assumed which can already give rise to interesting physics.

In order to find the phonon spectrum for the general case one can make use of the convenient method provided in [50]. In brief, one expands the Hamiltonian up to the second order around the equilibrium configuration. Then each ion can be associated with its local harmonic oscillator frequency defined as $\Omega_j = \sqrt{\frac{V_{jj}}{M}}$, where $V_{ij} = \frac{\partial^2 V}{\partial(\delta R_i)\partial(\delta R_j)}$ is the second derivative of the total potential energy calculated at equilibrium and M denotes the mass of the ion, while δR_j is the small displacement of the j-th ion from its equilibrium position. In the next step one introduces local ladder operators corresponding to these local oscillators and rewrites the Hamiltonian. The latter acquires quadratic form and can be diagonalized using a generalized Bogoliubov transformation, leading to the canonical phonon mode structure

$$\hat{H}_{\mathrm{ion}} = \sum_m \hbar\omega_m \hat{b}_m^\dagger \hat{b}_m \tag{16}$$

with ω_m being the energy of the m-th collective mode, and $\hat{b}_m$, $\hat{b}_m^\dagger$ denoting the phonon creation and annihilation operators that fulfill the usual bosonic commutation relations.

The atomic band structure is determined by the interaction with the static ion chain. Although the ion-atom interaction has a rather long-range character $V_{\mathrm{a-i}}(r) = -C^4/r^4$ with the characteristic range $R^\star$ being of the order of few thousand Bohr radii, here the typical length scales of the lattice are much larger than the interaction range and it is sufficient to make use of the one-dimensional pseudopotential approximation

$$V_{\mathrm{a-i}}(x) = g^e\delta(x) + g^o\delta'(x)\partial_\pm \tag{17}$$

with coefficients g^e, g^o describing the interaction in the even and odd partial waves (one-dimensional analogues of the three-dimensional case). The action of the operator on the right of Eq. (17) on a test function is defined as $2\,\hat{\partial}_\pm\psi(x) = [\psi'(0^+) + \psi'(0^-)]$ with $\psi'(0^\pm) = \lim_{x\to 0^\pm}\psi'(x)$, where the apex $'$ denotes the spatial derivative. Usually the even part of the interaction is expected to dominate. The resulting lattice potential $V_{\mathrm{lat}}(x) = \sum V_{\mathrm{a-i}}(x - R_0^{(i)})$

gives rise to a band structure which can be calculated numerically. In addition to this, the atoms interact with each other via van der Waals forces which have local character described by a pseudopotential similar to (17). One can then switch to the basis consisting of maximally localized Wannier states in which the atomic part of the Hamiltonian takes the familiar form of the fermionic Hubbard model.

The crucial element for the simulation of polaron models is the coupling of the atoms to the phonons which results from the ion-atom interaction beyond the static ion approximation. Following the condensed matter theory textbooks, one can expand the atom-ion interaction to the first nonvanishing order with respect to the ions' equilibrium positions. in the same way as the ionic Hamiltonian, obtaining the atom-phonon interaction $V_{\mathrm{a-ph}}(x)$ as a correction to $V_{\mathrm{lat}}(x)$. The atom-phonon coupling is then by definition given as

$$\hat{H}_{\mathrm{a-ph}} = \int d\mathbf{r}\hat{\rho}(\mathbf{r})V_{\mathrm{a-ph}}(\mathbf{r}) \tag{18}$$

with $\hat{\rho}(\mathbf{r})$ denoting the atomic density operator. After some algebraic transformations, the total Hamiltonian of the system can be written as

$$\begin{aligned}\hat{H} = -\sum_{ij} J_{ij}\hat{c}^{\dagger}_{i\sigma}\hat{c}_{j\sigma} + \sum_{i} U\hat{n}_{i\uparrow}\hat{n}_{i\downarrow} + \sum_{ij\sigma\sigma'} V_{ij}\hat{n}_{i\sigma}\hat{n}_{j\sigma'} + \\ + \sum_{m}\omega_m\hat{b}^{\dagger}_m\hat{b}_m + \sum_{ij\sigma} M_{il}\hat{n}_{i\sigma}\hat{x}_l\,,\end{aligned} \tag{19}$$

with $\hat{x}_l = \hat{a}_l + \hat{a}^{\dagger}_l$. Note the presence of the two types of phonon operators $\hat{a}$, $\hat{b}$ connected with each other via $hata_j = \sum_m (u^m_j - v^m_j)\hat{b}_m$ and the u_j, v_j parameters being diagonalization coefficients. The operators $\hat{a}$ have local character, in contrast to the collective modes described with $\hat{b}$. The atom-phonon coupling coefficient written in terms of local operators and Wannier states reads

$$M_{nj} = \sqrt{\frac{\hbar}{2MN\Omega_j}}\frac{1}{\sqrt{N}}\sum_k \alpha(k)e^{ikR_{nj}}|k|V_{e-i}(k)\,, \tag{20}$$

and can have local (onsite) or finite range character.

It is now convenient to perform the generalized Lang-Firsov transformation $\overline{H} = e^S H e^{-S}$ [51, 52] defined by the generator

$$\hat{S} = i\sum_{i,j}\lambda_{ij}\hat{n}_i(\hat{a}_j - \hat{a}^{\dagger}_j)\,, \tag{21}$$

with λ being an arbitrary number. This transformation dresses the atomic movement with lattice distortions. These new quasiparticles are called polarons. It is possible to choose λ such that the atom-phonon coupling term vanishes, and instead phonon-mediated interactions between the polarons emerge. The tunneling term becomes strongly suppressed, indicating that polarons typically have low mobility. The exemplary effective interaction is shown in Figure 12. As it turns out, for the chosen set of parameters the interactions are nonlocal and the particles attract each other weakly on long length scales. This is due to the fact that in this particular case the effective interaction is mediated mainly by the lowest phonon mode of the ionic lattice and reflects its shape.It is also possible to realize local effective attraction that would merely renormalize the onsite atomic repulsion. The system is thus suitable for quantum simulation of extended Hubbard-Holstein model. Experimentally available control knobs can allow for reaching different regimes. This is especially relevant as numerical methods for studying the phase diagram and the out-of-equilibrium dynamics of such models turn out to be challenging.

4.11 Summary

The works forming the cycle of publications described above bring insight into fundamental collisional properties of cold atoms and ions, in particular in the presence of an external confining potential. Building on this basis, new protocols for precision measurements, magnetometry, and quantum simulations have been introduced. Microscopic understanding of few-body physics in these systems is crucial for developing efficient theoretical models for the many-body dynamics.

In the coming years, I plan to extend the results obtained for ion-atom systems, especially by going beyond two-body effects. This includes three-body recombination and the role of strong many-body correlations in transport. The other promising direction is to explore applications of cold atomic systems in quantum technologies, especially quantum simulations. Emerging experimental platforms such as optical tweezer setups which are particularly exciting in that regard will require including the role of strong optical confinement with much higher precision than current theoretical proposals. In general, the interplay between strong interactions and geometrical constraints strongly connects the AMO and condensed matter systems. I aim to explore these links, looking for suitable atomic systems for quantum simulations of various nonequilibrium phenomena as well as adapting the few-body methods developed for atoms and molecules to the physics of quasiparticles such as excitons and exciton-polaritons.

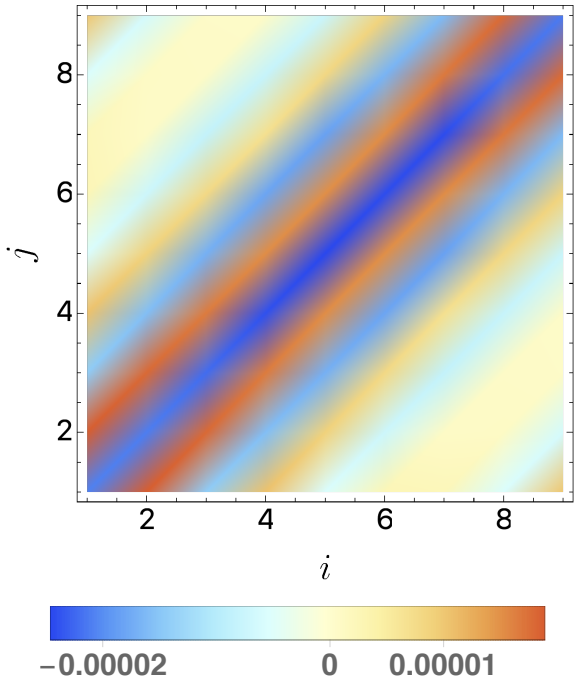

Figure 12: The effective interaction between the polarons after the Lang-Firsov transformation for the atom-ion even scattering length $a_e = 0.008R^\star$ and the ion spacing $d = 15R^\star$. From [H4].

5 Presentation of significant scientific activity conducted at more than one institution

The research described in the previous sections has been conducted mainly during postdoctoral research stays at the University of Stuttgart and Forschungszentrum Jülich in Germany, in collaboration with the experimental group in Stuttgart as well as with renowned scientists from various international institutions. Part of this research [H4] has been initiated during an extended visit at the University of Harvard. Other research projects not included in the main scientific achievement which also often result from international collaborations are listed below in reverse chronological order.

B.1 J. Kumlin, K. Jachymski, H. P. Büchler, *Beyond mean-field corrections for dipolar bosons in an optical lattice*, Phys. Rev. A 99, 033622 (2019)

B.2 M. Tomza, K. Jachymski, R. Gerritsma, A. Negretti, T. Calarco, Z. Idziaszek, P. S. Julienne, *Cold hybrid ion-atom systems*, Rev. Mod. Phys. 91, 035001 (2019)

B.3 K. Jachymski, R. Ołdziejewski, *Nonuniversal beyond-mean-field properties of quasi-two-dimensional dipolar Bose gases*, Phys. Rev. A 98, 043601 (2018)

B.4 M. Sroczyńska, T. Wasak, K. Jachymski, T. Calarco, Z. Idziaszek, *Trap-induced shape resonances in an ultracold few-body system of an atom and static impurities*, Phys. Rev. A 98, 012708 (2018)

B.5 K. Jachymski, F. Meinert, H. Veksler, P. S. Julienne, S. Fishman, *Ultracold atoms in quasi-one-dimensional traps: A step beyond the Lieb-Liniger model*, Phys. Rev. A 95, 052703 (2017)

B.6 B. Drews, M. Deiss, K. Jachymski, Z. Idziaszek, J. Hecker Denschlag, *Inelastic collisions of ultracold triplet Rb2 molecules in the rovibrational ground state*, Nature Communications 8, 14854 (2017)

B.7 K. Jachymski, M. Hapka, J. Jankunas, A. Osterwalder, *Experimental and theoretical studies of low energy Penning ionization of NH3, CH3F and CHF3*, ChemPhysChem 17, 3776 (2016)

B.8 J. Jankunas, K. Jachymski, M. Hapka, A. Osterwalder, *Importance of rotationally inelastic processes in low-energy Penning ionization of CHF3*, Journ. Chem. Phys. 144, 221102 (2016)

B.9 K. Jachymski, P. Bienias, H. P. Büchler, *Three-body interactions of Rydberg slow light polaritons*, Phys. Rev. Lett. 117, 053601 (2016)

B.10 T. Maier, I. Ferrier-Barbut, H. Kadau, M. Schmitt, M. Wenzel, C. Wink, T. Pfau, K. Jachymski and P.S.Julienne, *Broad universal Feshbach resonances in the chaotic spectrum of dysprosium atoms*, Phys. Rev. A 92, 060702(R) (2015)

B.11 K. Jachymski, P. S. Julienne, *Chaotic scattering in the presence of densely overlapping Feshbach resonances*, Phys. Rev. A 92, 020702(R) (2015)

B.12 J. Jankunas, K. Jachymski, M. Hapka and A. Osterwalder, *Observation of orbiting resonances in the NH3+He(3S1) Penning ionization*, Journ. Chem. Phys. 142, 164305 (2015)

B.13 Z. Idziaszek, K. Jachymski and P. S. Julienne, *Reactive collisions in confined geometries*, New Journ. Phys. 17, 035007 (2015)

B.14 A. Simoni, S. Srinivasan, J. M. Launay, Z. Idziaszek, K. Jachymski, P. S. Julienne, *Polar molecule reactive collisions in quasi-1D systems*, New Journ. Phys. 17, 013020 (2015)

B.15 K. Jachymski, M. Krych, P. S. Julienne and Z. Idziaszek, *Quantum defect model of a reactive collision at finite temperature*, Phys. Rev. A 90, 042705 (2014)

B.16 J. Jankunas, B. Bertsche, K. Jachymski, M. Hapka and A. Osterwalder, *Dynamics of gas phase Ne*-NH3 and Ne*-ND3 Penning ionization at low temperatures*, J. Chem. Phys. 140, 244302 (2014)

B.17 K. Jachymski, Z. Idziaszek and T. Calarco, *Fast quantum gate via Feshbach-Pauli blocking in a nanoplasmonic trap*, Phys. Rev. Lett. 112, 250502 (2014)

B.18 K. Jachymski and P. S. Julienne, *Analytical model of overlapping Feshbach resonances*, Phys. Rev. A 88, 052701 (2013)

B.19 K. Jachymski, M. Krych, P. S. Julienne and Z. Idziaszek, *Quantum theory of reactive collisions for $1/r^n$ potentials*, Phys. Rev. Lett. 110, 213202 (2013)

B.20 K. Jachymski, Z. Idziaszek, T. Calarco, *Feshbach resonances in a nonseparable trap*, Phys. Rev. A 87, 042701 (2013)

B.21 K. Jachymski, Z. Idziaszek, *Off-resonant light scattering from ultracold gases in optical lattices*, Eur. Phys. J. Special Topics 217, 85-90 (2013)

B.22 K. Jachymski, Z. Idziaszek, *Light scattering from ultracold gases in disordered optical lattices*, Phys. Rev. A 86, 023607 (2012)

5.1 Description of other scientific achievements

Articles [B22,B21] contain the results of my Master thesis prepared under supervision of dr hab. Zbigniew Idziaszek. The main goal of the project was to find a nondestructive way to detect Anderson localization in disordered optical lattices. It has been shown that off-resonant light scattering can be used for this purpose even at finite temperatures.

My PhD thesis, which was prepared within the International PhD studies framework, focused on low energy collisions of atoms as well as molecules, in particular the properties of chemical reactions in the ultracold regime. The main tool used in the studies has been the Multichannel Quantum Defect Theory (MQDT), which allows for efficient and general description of scattering. Works [B19,B15] study different aspects of inelastic processes for power-law interaction potentials such as Wigner threshold laws and shape resonances. The results have been further extended to include the presence of external confining potential which effectively reduces the dimensionality [B14,B13,B5]. Another important topic on which I have been working jointly with prof. Paul Julienne are overlapping Feshbach resonances which appear in systems with multiple closed channels, which is especially relevant for more complex atoms as well as atom-molecule collisions. Their properties have been studied in [B18,B11]. These results created an opportunity to collaborate with the experimental group of prof. Andreas Osterwalder on the topic of Penning ionization of polyatomic molecules by metastable noble gas atoms in a range of collision energies. The results of this joint project were published in works [B16,B12,B8,B7]. Further experimental collaborations include work [B6] with the group of Johannes Hecker Denschlag on reactive collisions of Rb_2 molecules in a quasi-1D setup and with the group of Tilman Pfau on Feshbach resonances in dysprosium [B10].

Furthermore, articles [B20,B4] study the basic properties of tightly confined systems and the interplay between trap-induced shape Feshbach resonances. The results have been used to develop a simple quantum gate protocol [B17] in which a Feshbach resonance prevents a pair of fermionic atoms from populating certain states that would lead to decreased gate fidelity.

During my postdoctoral stay in Stuttgart as a Humboldt fellow I studied the few-body properties of Rydberg polaritons which are quasiparticles composed of a photon and a Rydberg excitation. Some of the results were published in [B9]. Furthermore, I became interested by the concept of quantum droplets which are formed due to beyond mean-field effects. Works [B1,B3] study the properties of dipolar droplets in the presence of an external confining potential such as an optical lattice. The main objective has been to go beyond the commonly used local density approximation which can only be applied if the trap length scales are much larger than the condensate healing length.

The review paper [B2] is devoted to the physics of ion-atom hybrid systems which are discussed in detail in the previous section. As this paper does not contain new scientific results, it has been left out of the main scientific achievement.

6 Teaching, organizational and popularization activity

Teaching experience

The applicant has so far supervised three students: one Bachelor student in Warsaw, one in Stuttgart and one Master student in Cologne. The teaching experience of the applicant includes

- 2019 tutorials for Quantum Information Processing lecture (University of Cologne, in English)
- 2018 co-supervisor of the Hauptseminar "Quantum gases and liquids" (University of Stuttgart, in English)
- 2016/17 lecture on Advanced Quantum Mechanics (University of Stuttgart, in English, jointly with prof. Maria Daghofer)
- 2016 co-supervisor of the Hauptseminar "Ultracold quantum gases" (University of Stuttgart, in English)
- 2015/16 tutorials for Advanced Quantum Mechanics (University of Stuttgart, in English)
- 2014/15 tutorials for Mathematical Analysis (University of Warsaw, in Polish)
- 2014/15 tutorials for Algebra (University of Warsaw, in Polish)
- 2012/13 tutorials for Quantum Mechanics and Quantum Chemistry (University of Warsaw, in Polish)
- 2011/12 tutorials for Differential and Integral Calculus (University of Warsaw, in Polish)

Popularization

In 2019 the applicant gave a popular lecture for high school students in Technical University High School in Łódź on the bascis of quantum mechanics and emerging quantum technologies. In 2020 the applicant gave an online seminar for the SKN "Nanorurki".

References

[1] Maciej Lewenstein, Anna Sanpera, Veronica Ahufinger, Bogdan Damski, Aditi Sen, and Ujjwal Sen. Ultracold atomic gases in optical lattices: mimicking condensed matter physics and beyond. *Advances in Physics*, 56(2):243–379, 2007.

[2] Antonio Acín, Immanuel Bloch, Harry Buhrman, Tommaso Calarco, Christopher Eichler, Jens Eisert, Daniel Esteve, Nicolas Gisin, Steffen J Glaser, Fedor Jelezko, et al. The quantum technologies roadmap: a european community view. *New Journal of Physics*, 20(8):080201, 2018.

[3] Christopher J Pethick and Henrik Smith. *Bose–Einstein condensation in dilute gases*. Cambridge university press, 2008.

[4] Dirk Van Delft and Peter Kes. The discovery of superconductivity. *Physics Today*, 63(9):38–43, 2010.

[5] J. Bardeen, L. N. Cooper, and J. R. Schrieffer. Theory of superconductivity. *Phys. Rev.*, 108:1175–1204, Dec 1957.

[6] Wolfgang Demtröder. *Laser spectroscopy: basic concepts and instrumentation.* Springer Science & Business Media, 2013.

[7] Arthur Ashkin. Trapping of atoms by resonance radiation pressure. *Physical Review Letters*, 40(12):729, 1978.

[8] E. L. Raab, M. Prentiss, Alex Cable, Steven Chu, and D. E. Pritchard. Trapping of neutral sodium atoms with radiation pressure. *Phys. Rev. Lett.*, 59:2631–2634, Dec 1987.

[9] Mike H Anderson, Jason R Ensher, Michael R Matthews, Carl E Wieman, and Eric A Cornell. Observation of bose-einstein condensation in a dilute atomic vapor. *science*, 269(5221):198–201, 1995.

[10] K. B. Davis, M. O. Mewes, M. R. Andrews, N. J. van Druten, D. S. Durfee, D. M. Kurn, and W. Ketterle. Bose-einstein condensation in a gas of sodium atoms. *Phys. Rev. Lett.*, 75:3969–3973, Nov 1995.

[11] Dale G Fried, Thomas C Killian, Lorenz Willmann, David Landhuis, Stephen C Moss, Daniel Kleppner, and Thomas J Greytak. Bose-einstein condensation of atomic hydrogen. *Physical Review Letters*, 81(18):3811, 1998.

[12] Svetlana Kotochigova. Controlling interactions between highly magnetic atoms with feshbach resonances. *Reports on Progress in Physics*, 77(9):093901, 2014.

[13] Michał Tomza, Krzysztof Jachymski, Rene Gerritsma, Antonio Negretti, Tommaso Calarco, Zbigniew Idziaszek, and Paul S. Julienne. Cold hybrid ion-atom systems. *Rev. Mod. Phys.*, 91:035001, Jul 2019.

[14] Goulven Quemener and Paul S Julienne. Ultracold molecules under control! *Chemical Reviews*, 112(9):4949–5011, 2012.

[15] Iulia M Georgescu, Sahel Ashhab, and Franco Nori. Quantum simulation. *Reviews of Modern Physics*, 86(1):153, 2014.

[16] Markus Greiner, Olaf Mandel, Tilman Esslinger, Theodor W Hänsch, and Immanuel Bloch. Quantum phase transition from a superfluid to a mott insulator in a gas of ultracold atoms. *Nature*, 415(6867):39–44, 2002.

[17] Luca Pezzè, Augusto Smerzi, Markus K. Oberthaler, Roman Schmied, and Philipp Treutlein. Quantum metrology with nonclassical states of atomic ensembles. *Rev. Mod. Phys.*, 90:035005, Sep 2018.

[18] Cheng Chin, Rudolf Grimm, Paul Julienne, and Eite Tiesinga. Feshbach resonances in ultracold gases. *Reviews of Modern Physics*, 82(2):1225, 2010.

[19] Herman Feshbach. Unified theory of nuclear reactions. *Annals of Physics*, 5(4):357–390, 1958.

[20] Manfred Mark, Florian Meinert, Katharina Lauber, and Hanns-Christoph Nägerl. Mott-insulator-aided detection of ultra-narrow feshbach resonances. *SciPost Phys*, 5:055, 2018.

[21] Jessie T. Zhang, Yichao Yu, William B. Cairncross, Kenneth Wang, Lewis R. B. Picard, Jonathan D. Hood, Yen-Wei Lin, Jeremy M. Hutson, and Kang-Kuen Ni. Forming a single molecule by magnetoassociation in an optical tweezer. *Phys. Rev. Lett.*, 124:253401, Jun 2020.

[22] J. D. Hood, Y. Yu, Y.-W. Lin, J. T. Zhang, K. Wang, L. R. Liu, B. Gao, and K.-K. Ni. Multichannel interactions of two atoms in an optical tweezer. *Phys. Rev. Research*, 2:023108, Apr 2020.

[23] Thomas Busch, Berthold-Georg Englert, Kazimierz Rzażewski, and Martin Wilkens. Two cold atoms in a harmonic trap. *Foundations of Physics*, 28(4):549–559, 1998.

[24] Félix Werner and Yvan Castin. General relations for quantum gases in two and three dimensions. ii. bosons and mixtures. *Phys. Rev. A*, 86:053633, Nov 2012.

[25] T. Lahaye, J. Metz, B. Fröhlich, T. Koch, M. Meister, A. Griesmaier, T. Pfau, H. Saito, Y. Kawaguchi, and M. Ueda. *d*-wave collapse and explosion of a dipolar bose-einstein condensate. *Phys. Rev. Lett.*, 101:080401, Aug 2008.

[26] Holger Kadau, Matthias Schmitt, Matthias Wenzel, Clarissa Wink, Thomas Maier, Igor Ferrier-Barbut, and Tilman Pfau. Observing the rosensweig instability of a quantum ferrofluid. *Nature*, 530(7589):194–197, 2016.

[27] Igor Ferrier-Barbut, Holger Kadau, Matthias Schmitt, Matthias Wenzel, and Tilman Pfau. Observation of quantum droplets in a strongly dipolar bose gas. *Physical review letters*, 116(21):215301, 2016.

[28] Aristeu RP Lima and Axel Pelster. Beyond mean-field low-lying excitations of dipolar bose gases. *Physical Review A*, 86(6):063609, 2012.

[29] S Yi and L You. Trapped atomic condensates with anisotropic interactions. *Physical Review A*, 61(4):041604, 2000.

[30] Fabian Böttcher, Matthias Wenzel, Jan-Niklas Schmidt, Mingyang Guo, Tim Langen, Igor Ferrier-Barbut, Tilman Pfau, Raúl Bombín, Joan Sánchez-Baena, Jordi Boronat, et al. Dilute dipolar quantum droplets beyond the extended gross-pitaevskii equation. *Physical Review Research*, 1(3):033088, 2019.

[31] M. Olshanii. Atomic scattering in the presence of an external confinement and a gas of impenetrable bosons. *Phys. Rev. Lett.*, 81:938, 1998.

[32] Harald Cramér. *Mathematical methods of statistics*, volume 43. Princeton university press, 1999.

[33] Vittorio Giovannetti, Seth Lloyd, and Lorenzo Maccone. Quantum metrology. *Physical review letters*, 96(1):010401, 2006.

[34] Thomas F O'Malley, Larry Spruch, and Leonard Rosenberg. Modification of effective-range theory in the presence of a long-range (r- 4) potential. *Journal of Mathematical Physics*, 2(4):491–498, 1961.

[35] John R Taylor. *Scattering theory: the quantum theory of nonrelativistic collisions*. Courier Corporation, 2006.

[36] LD Landau and SI Pekar. Effective mass of a polaron. *Zh. Eksp. Teor. Fiz*, 18(5):419–423, 1948.

[37] André Schirotzek, Cheng-Hsun Wu, Ariel Sommer, and Martin W Zwierlein. Observation of fermi polarons in a tunable fermi liquid of ultracold atoms. *Physical Review Letters*, 102(23):230402, 2009.

[38] Nils B Jørgensen, Lars Wacker, Kristoffer T Skalmstang, Meera M Parish, Jesper Levinsen, Rasmus S Christensen, Georg M Bruun, and Jan J Arlt. Observation of attractive and repulsive polarons in a bose-einstein condensate. *Physical Review Letters*, 117(5):055302, 2016.

[39] Pietro Massignan, Matteo Zaccanti, and Georg M Bruun. Polarons, dressed molecules and itinerant ferromagnetism in ultracold fermi gases. *Reports on Progress in Physics*, 77(3):034401, 2014.

[40] F Grusdt and E Demler. New theoretical approaches to bose polarons. *Quantum Matter at Ultralow Temperatures*, 191:325, 2015.

[41] E.P Gross. Motion of foreign bodies in boson systems. *Annals of Physics*, 19(2):234 – 253, 1962.

[42] Robin Cote, V Kharchenko, and MD Lukin. Mesoscopic molecular ions in bose-einstein condensates. *Physical Review Letters*, 89(9):093001, 2002.

[43] P Massignan, Christopher J Pethick, and H Smith. Static properties of positive ions in atomic bose-einstein condensates. *Physical Review A*, 71(2):023606, 2005.

[44] H. Fröhlich. Electrons in lattice fields. *Adv. Phys.*, 3(11):325–361, 1954.

[45] Martin Hohenadler and Wolfgang von der Linden. Lang-firsov approaches to polaron physics: From variational methods to unbiased quantum monte carlo simulations. In *Polarons in Advanced Materials*, pages 463–502. Springer, 2007.

[46] Jozef T Devreese and Alexandre S Alexandrov. Fröhlich polaron and bipolaron: recent developments. *Rep. Prog. Phys.*, 72(6):066501, 2009.

[47] A Alexandrov and J Ranninger. Bipolaronic superconductivity. *Physical Review B*, 24(3):1164, 1981.

[48] U. Bissbort, D. Cocks, A. Negretti, Z. Idziaszek, T. Calarco, F. Schmidt-Kaler, W. Hofstetter, and R. Gerritsma. Emulating solid-state physics with a hybrid system of ultracold ions and atoms. *Phys. Rev. Lett.*, 111:080501, 2013.

[49] Shmuel Fishman, Gabriele De Chiara, Tommaso Calarco, and Giovanna Morigi. Structural phase transitions in low-dimensional ion crystals. *Phys. Rev. B*, 77:064111, Feb 2008.

[50] U. Bissbort, W. Hofstetter, and D. Poletti. Operator-based derivation of phonon modes and characterization of correlations for trapped ions at zero and finite temperature. *Phys. Rev. B*, 94:214305, Dec 2016.

[51] IG Lang and Yu A Firsov. Kinetic theory of semiconductors with low mobility. *Sov. Phys. JETP*, 16(5):1301, 1963.

[52] Martin Hohenadler, Hans Gerd Evertz, and Wolfgang von der Linden. Quantum monte carlo and variational approaches to the holstein model. *Phys. Rev. B*, 69:024301, Jan 2004.